frontiers in Materials

ORIGINAL RESEARCH
published: 28 June 2021
doi: 10.3389/fmats.2021.687282

Characterizing Biaxially Stretched Polypropylene / Graphene Nanoplatelet Composites

*B. Mayoral[1], G Menary[1], P Martin[1], G Garrett[1], B Millar[1], P Douglas[1], N. Khanam[2], M. A. AlMaadeed[2,3], M. Ouederni[4], A. Hamilton[1,5] and D. Sun[1]**

[1]School of Mechanical and Aerospace Engineering, Queen's University Belfast, Belfast, United Kingdom, [2]Center for Advanced Materials, Qatar University, Doha, Qatar, [3]Materials Science and Technology Program, Qatar University, Doha, Qatar, [4]Qatar Petrochemical Company, Doha, Qatar, [5]School of Engineering and the Environment, University of Southampton, Southampton, United Kingdom

In this work, polypropylene (PP) nanocomposites containing different weight concentration of graphene nanoplatelets (GNP) were prepared by melt-mixing using an industrial-scale, co-rotating, intermeshing, twin-screw extruder. The materials were then compression moulded into sheets, and biaxially stretched at different stretching ratios (SRs) below the PP melting temperature. The effects of GNP content and biaxial stretching on the bulk properties of unfilled PP and PP/GNP nanocomposites have been investigated in details. Results show that the addition of GNP (>5wt%) can lead to electrically conductive composites due to the formation of percolation network. The GNP have led to increased polymer crystallinity and enhanced materials stiffness and strength. Biaxial stretching process further enhances the materials mechanical properties but has slightly decreased the composites electrical conductivity. The PP/GNP nanocomposites were also processed into 3D demonstrator parts using vacuum forming, and the properties of which were comparable with biaxially stretched composites.

Keywords: polymer composites, graphene nanoplatelet, Bi-axial stretching, mechanical properties, thermal properties, electrical properties

Edited by:
Miroslav Slouf,
Institute of Macromolecular Chemistry (ASCR), Czechia

Reviewed by:
Jose Antonio Covas,
University of Minho, Portugal
John Zhanhu Guo,
, University of Tennessee, United States

****Correspondence:***
D. Sun
d.sun@qub.ac.uk

Specialty section:
This article was submitted to Polymeric and Composite Materials, a section of the journal Frontiers in Materials

Received: *29 March 2021*
Accepted: *10 June 2021*
Published: *28 June 2021*

Citation:
Mayoral B, Menary G, Martin P, Garrett G, Millar B, Douglas P, Khanam N, AlMaadeed MA, Ouederni M, Hamilton A and Sun D (2021) Characterizing Biaxially Stretched Polypropylene / Graphene Nanoplatelet Composites. Front. Mater. 8:687282. doi: 10.3389/fmats.2021.687282

INTRODUCTION

Graphene possesses exceptional mechanical properties, excellent thermal/electrical conductivity as well as large specific surface area. Due to its outstanding multifunctional properties, graphene has received extensive research interests in recent years in multiple fields (Zhao et al., 2019; Jiang et al., 2020; Noorunnisa et al., 2016a; Noorunnisa et al., 2016b; Nidamanuri et al., 2020; Zhao et al., 2020; Zhou et al., 2021). Compared to single-layer graphene, large yield of graphene nanoplatelets (GNP) can be produced from natural graphite precursors at a lower cost (Noorunnisa et al., 2016a). Past literatures suggest the electrical conductivity and mechanical properties of polymers can be greatly enhanced by the addition of GNP due to its high electrical conductivity and excellent mechanical properties (modulus 1 TPa for graphene (Mayoral et al., 2015). For instance, GNP have been used to reinforce a range of polymers such as polyethylene (Noorunnisa et al., 2016b), polyethylene terephthalate (Zhang et al., 2010), polycarbonate (King et al., 2011), thermoplastic polyurethane (Yuan et al., 2017), polyether ether ketone (He et al., 2020; Zhu et al., 2021) and polyamide (Mayoral et al., 2015), etc, to obtain various nanocomposites with enhanced thermal, mechanical and electrical properties. Polypropylene (PP) is one of the commonly used matrix materials for polymer composites due to its availability and ease of processing (Maddah, 2016). PP has a low density

and high crystallinity in comparison with other engineering thermoplastics, allowing for potential weight reductions of the final products. Its excellent heat resistance, moisture barrier, and good optical properties also enable its wide industrial applications in packaging, laboratory equipment, automotive components and many others (Valentini et al., 2003; Xu et al., 2019; Tsai, 2020; Yan et al., 2020; Singh, 2021). In recent years, GNP reinforced PP nanocomposites have received increasing research interest. For instance, Liang and Du (2018) investigated the effect of GNP concentration on the melt flow behavior and flexural properties of reinforced PP composites. An optimum concentration of 0.4wt% has been reported for maximum mechanical resistance and a linear correlation between the melt shear viscosity and GNP weight fraction. Jun et al. (2018a) studied the effect of GNP size on PP nanocomposites processed by twin-screw extrusion and injection molding and found that smaller size GNP (<25 μm) are more effective in improving the composites tensile strength and thermal stabilities, due to their lower tendency to agglomeration. Jun et al. (2018b) also reported large sized GNP (>150 μm) can reduce the GNP percolation threshold and increase electrical conductivity of the melt compounded PP/GNP nanocomposite. Similar result was also reported by He et al. (2017a) in extruded and compression molded PP/GNP nanocomposites. He et al. (2017b) also reported that the residence time during extrusion plays an important role in dispersing GNP and better dispersion of GNP tends to increase the electrical and thermal conductivities of the resulting PP/GNP nanocomposites and significantly reduce the electrical percolation threshold.

From the literature, it can be seen that the processing route used to manufacture PP/GNP nanocomposites is likely to have a large impact on the dispersion and orientation of GNP, and consequently influence the properties of the resulting composite materials. In practical applications, polymer composites produced through primary processing (such as extrusion, injection molding) may require secondary processing in order to be made into final products. During secondary processes such as thermoforming and blow molding, heated polymer materials are subjected to rapid biaxial deformation as they are drawn into the shape of a mold (Martin et al., 2005). The effects of the biaxial stretching action and the presence of the filler materials on the resulting structure and properties of stretched PP/GNP composites is yet to be explored. In the present work, PP/GNP nanocomposites were prepared *via* melt-mixing using an industrial co-rotating, intermeshing extruder with custom-designed twin-screw. Compression moulded PP/GNP sheets were subsequently subjected to bi-axial stretching and the effects of GNP addition and different biaxial stretching ratios on the resulting composites properties have been investigated. Demonstrator parts were produced using vacuum forming process and the properties of the biaxially stretched material and the demonstrator parts have been compared.

METHODS

Materials

Moplen HP500N grade Polypropylene (Homopolymer, Melt Flow Rate (230°C/2.16 kg) = 12 g/10 min, density = 0.90 g/cm^3) was supplied by Basell. Grade M xGNP® GNP are made through a proprietary manufacturing process, and were supplied by XG Sciences. The technical specifications for the xGNP® grade M GNP are detailed in **Table 1**.

Melt-Mixing of PP/GNP

In order to obtain better GNP dispersion in the polymer matrix, the as purchased PP pellets were cryogenically ground into micron scale fine powder using a Wedco SE-12 UR pilot plant grinding mill at 7,000 rpm and a gap size of 400 μm. Liquid nitrogen was used for temperature regulation in order to prevent shear heating and degradation of the materials. PP and GNP, both in powder form were mixed using a Thermo Scientific Prism Pilot three High Speed Mixer at 2000rpm for 2 min.

The melt-mixing process was performed using a co-rotating intermeshing twin-screw extruder (Collin GmbH) with a screw diameter of 25 mm and a barrel length of 750 mm (L/D = 30). A bespoke screw configuration designed in-house (Mayoral et al., 2014) was used to enhance the nanoparticle dispersion into the polymer matrix. The detailed configuration of the twin-screw extruder can be found in (Mayoral et al., 2015). In brief, this configuration consists of forward conveying and forward kneading block elements with the addition of a toothed mixing element into the mixing zone and a reverse conveying element after the mixing zone. On exiting the capillary die, the extrudate was drawn through a cooled water bath at a constant haul off rate and pressure. The extrudate was dried by passing through an air ring and then pelletized using a Collin Pelletiser. The process parameters for PP/GNP twin-screw extrusion are: feeding rate = 2.5 kg/h, screw speed = 150 rpm, residence time = 1 min 30 s. Additional process parameters can be found in **Table 2**. According to the published literature, electrical percolation network within PP/GNP composite can be achieved at 5–10wt% GNP concentration (He et al., 2017). Given the bi-axial stretching process may potentially increase the mean distance between conductive filler materials (Feng and Jiang, 2014) and increase the percolation threshold, GNP weight concentrations of 0, 5, 10, 15, and 20wt% were deployed and the resulting composites were named as PP unfilled, PP/5%M-5, PP/10%M-5, PP/15%M-5, PP/20%M-5, respectively.

Compression Molding

The extruded pellets were dried in an oven at 80°C for 4 h before compression molding. Materials were compression moulded at 200°C at 150bars for 3 min using a Rondol platen press. Square samples with dimension of 12 mm × 12 mm × 1 mm were prepared for subsequent biaxial stretching tests.

Biaxial Stretching of PP/GNP Composites

The as purchased PP has a narrow softening temperature in the range 145–155°C. Trials show that the addition of GNP modified the PP thermal properties and that 147°C was the optimum temperature required for stretching the nanocomposite specimens. Test specimens were cut into 75 mm squares and were clamped using 24 nitrogen-driven pneumatic clamps of the biaxial stretching machine. More detailed configuration of the biaxial stretching machine can be found in (Martin et al., 2005;

TABLE 1 | XG Sciences xGNP® grade M GNP technical specifications.

Grade	Product	# Layers	Thickness (nm)	Diameter (μm)	Surf. Area (m^2/g)
M	M-5	18–24	6–8	5	120–150

TABLE 2 | Process parameters set for PP/GNP twin-screw extrusion.

PP/GNP	GNP	Pressure	Motor arrest	T_m
	wt (%)	Bar	Amp	°C
PP/M-5	5	3.2	13	218
	10	3.3	16	225
	15	3.5	17	227
	20	3.9	19	228

Zhang et al., 2020). It was found that only unfilled PP and PP/5wt % GNP can be successfully biaxially stretched to SR2. It was not possible to find a softening temperature suitable for stretching composite containing >10% GNP. This can be due to the higher GNP content has led to a high thermal conductivity of the PP/GNP composites, which rapidly dissipated the thermal energy, accelerated the crystallization process, and caused the very rapid cooling before it is possible to stretch the polymer (Martin et al., 2005). It is also found that the addition of GNP to PP limited the achievable strain rate to lower values and the best results were obtained for strain rate 2 s^{-1}. Therefore, a constant strain rate of 2 s^{-1} and stretch ratio (SR) of 1.5 and 2 was used to biaxially stretch the samples whenever possible and the true stress and nominal strain data were recorded.

Demonstrator Parts

Demonstrator products were developed for the targeted potential applications, such as enclosures with good mechanical robustness and electrostatic dissipation capabilities. Vacuum forming (C. R. Clarke 1820 Vacuum Former) was selected as the manufacturing process for producing 3D demonstrator prototypes. Optimized parameters used for vacuum molding were: 150°C/100 s for unfilled PP sheet and 150°C/76 s for PP/GNP composites sheet. Materials for static dissipation applications require an electrical resistivity of approximately 10^8 to 10^3 ohm-cm (King et al, 1999). The range of conductivity of the composites, and their ability to withstand biaxial deformation was first determined and the results were used to inform the formulation and dimension of the demonstrator parts. The thermal forming process and the resulting demonstrator parts are shown in **Supplementary Figures S2, S3**. The range of properties exhibited by the demonstrator parts were subsequently compared to those of the biaxially stretched materials, to evaluate the effectiveness of using biaxial stretching for product property prediction.

Mechanical Analysis

Tensile tests were carried out at room temperature following BS EN ISO 527–1: 1996 and using an Instron 5,564 universal Tester with a clip-on extensometer and a 2 kN load cell. Dumbbell-shaped samples (type 1BA) were cut from the compression moulded samples using a stamping press. For modulus measurement, nominal strain was determined using data from the extensometer, which was attached to the narrow portion of the dumb-bell samples, and at a crosshead speed of 1 mm/min. The elastic modulus was determined from the slope of the regression of the stress-strain data between 0.05–0.25% strain. For strength and elongation, the nominal strain was derived from the grip displacement at a crosshead speed of 50 mm/min.

Thermal Analysis

Differential scanning calorimetry (DSC) was performed to study the melting and crystallization behavior of unfilled PP and PP/GNP composites using a Perkin–Elmer DSC model six under an inert nitrogen atmosphere and a heating and cooling rate of 10 K/min, in a temperature range from 30 to 275°C. In all cases the samples were held at 275°C for 3 min, cooled to 30°C and reheated to 275°C to ensure complete melting of the crystalline fraction of PP and to remove thermal history. The apparent crystalline content of the PP composites was determined using a value of 148 J/g for the enthalpy of fusion for a theoretically 100% crystalline PP (Kaszonyiová et al., 2018).

Electrical Properties

Volume resistivity measurements were performed in accordance with ASTM D-257 on compression moulded and stretched specimens using a Keithley electrometer (Model 6517A) equipped with an 8,009 test fixture. Circular samples (Φ = 60 mm, t = 1 mm) was used. The sample was placed between two circular electrodes and the volume resistivity was measured by applying a DC voltage across opposite sides of the sample and measuring the resultant current through the sample.

Microstructural Analysis

The morphology and the degree of dispersion of GNPs in the polymer matrix were investigated using Scanning Electron Microscopy (SEM). Samples for SEM analysis were plasma

TABLE 3 | Effect of GNP addition on the thermal properties of unfilled PP and PP/GNP composites.

Material	First heating			Cooling		Second heating		
	Tm (°C)	X_c (%)	Impr (%)	Tc (°C)	Impr (%)	Tm (°C)	X_c (%)	Impr (%)
PP unfilled	168.6	40.41		108.2		167.7	39.26	
PP/5wt%M-5	169.2	61.49	52.17	122.9	13.59	169.1	60.14	53.18
PP/10wt% M-5	169.4	58.24	44.15	123.6	14.23	169.2	53.11	35.28
PP/15wt% M-5	169.6	57.36	41.97	124.1	14.70	169.8	49.73	26.68
PP/20wt% M-5	169.9	56.28	39.30	124.9	15.43	169.7	49.05	24.96

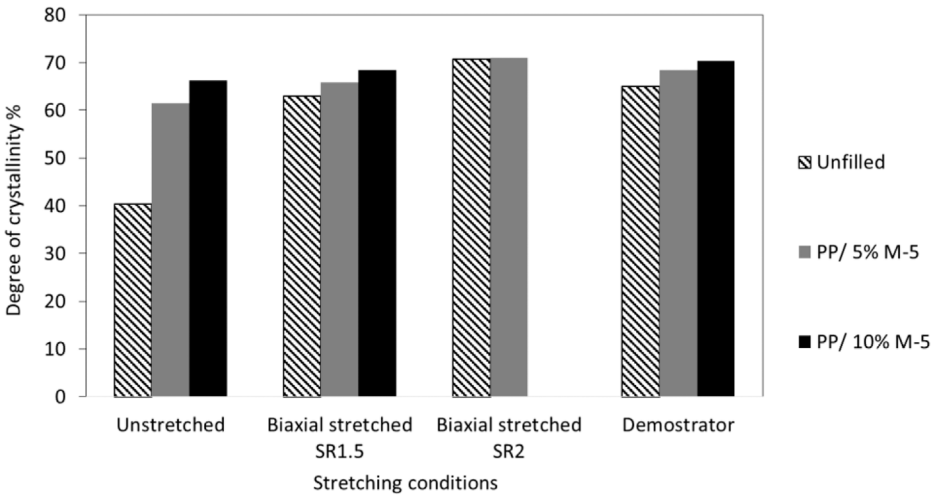

FIGURE 1 | Effect of GNP content and the biaxial stretching deformation on Xc% of unfilled PP, PP/GNP composites and the demonstrator parts.

etched for 60 s at an etching power of 100 w using a reactive ion etching system (STS Cluster C005) and then gold sputtered prior to imaging. These samples were examined using a JEOL 6500F Field Emission Scanning Electron Microscopy (FE-SEM) with an operating voltage of 5 kV.

RESULTS AND DISCUSSIONS

Thermal Properties

The melting and crystallization behavior of unfilled PP and PP/GNP composites were obtained based on the DSC data. **Table 3** shows the effect of GNP addition on the thermal properties of unfilled PP. The addition of GNP had little effect on the melting temperature (T_m) of PP. An increase in $\%X_c$ with increasing GNP content has been noticed, suggesting a change in the crystal type and the perfection. The presence of GNP is known to accelerate the PP crystallization kinetics (Beuguel et al., 2018), where GNP may serve as a nucleation site and PP chains may grow epitaxial on GNP (Jun et al., 2018). Similar behavior has also been reported in other polymer composite systems such as PA6/GNP composite (Mayoral et al., 2015).

Xc% of the testing materials (first heating) after biaxial deformation are given in **Figure 1** and more detailed data can be found in **Supplementary Table S1**. The results reflected a strain induced increase in crystallization, and a γ-β phase transition during the stretching process. Biaxial stretching of unfilled PP resulted in an increase in the crystallization temperature (T_c) of up to ~12 °C, depending on the SR. Significant increases in $X_c\%$ resulted from biaxial stretching, from ~40% (unstretched) to ~63% (SR1.5) and ~70% (SR2). This may be because as the strain rate increases, polymer chains have less time to relax leading to higher levels of chains orientation/alignment and thus higher degrees of strain-induced crystallization (Mayoral et al., 2013). No significant differences in T_g or T_m have been observed when the unfilled PP was biaxially deformed. For the PP/GNP composites, T_c increased by up to ~17 °C depending on the SR. The extent of $X_c\%$ increases is smaller as compared to unfilled PP. Under the same SR, the $X_c\%$ was similar for the unfilled PP and PP/GNP composites. The demonstrator parts showed similar Xc% with that of the biaxially stretched (SR1.5) neat PP and composite samples.

Mechanical Properties

The tensile mechanical properties of unfilled PP, PP/5%M-5 and PP/10% M-5 before and after biaxial deformation were presented in **Figure 2**. The typical stress-strain curves can be found in **Supplementary Figure S1**. Both Young's modulus and yield strength increased with the addition of GNP and with

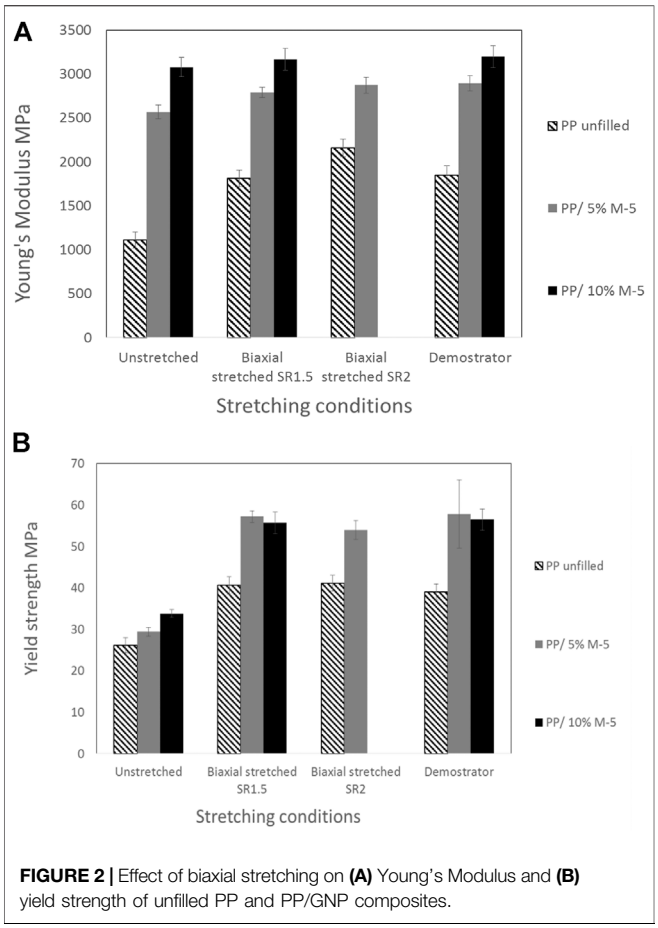

FIGURE 2 | Effect of biaxial stretching on **(A)** Young's Modulus and **(B)** yield strength of unfilled PP and PP/GNP composites.

increasing SR. The increase in Young's modulus due to stretching was most significant for unfilled PP, with SR giving ~2 fold increase in the Young's modulus. Such significant increase in stiffness may be attributed to the strong alignment of the crystalline region within the PP, producing more oriented chains in the stretching direction (Díez et al., 2005). This is also consistent with the crystallinity data shown in **Figure 1**, where biaxially stretched unfilled PP have greatly enhanced Xc%. In contrast, the effect of stretching on Young's moduli of PP/5% M-5 and PP/10% M-5 was less distinctive, as the presence of GNP has already led to significantly enhanced the composite crystallinity, and the Xc% change in these samples are less sensitive to stretching.

Figure 2B shows that biaxial stretching also resulted in increased yield strength for both unfilled PP and PP/GNP composites. The result is similar to the simulation results reported for biaxially stretched PP, where a higher yield stress observed as draw ratios increase was attributed to the increased crystalline structure orientation (Kershah et al., 2020). Enhanced yield strengths for PP/GNP composites may be due to the presence of GNP could have restricted the molecular chain mobility during the deformation process. In addition, the resulting yield strengths seen for unfilled PP and PP/5%M-5 are similar at SR1.5 and SR2. The mechanical properties measurements obtained for the demonstrator parts are in line with the results of the SR1.5 PP/GNP composites.

Electrical Properties

Figure 3 shows that the in-plane electrical resistivity of PP decreases 10^6 fold with addition of 10% GNP. This is due to the formation of the electrical percolation network, where the percolation threshold for PP/GNP system is reported to be ~5–10wt% (He et al., 2017; He et al., 2017). The electrical resistivity of PP/5%M-5 and PP/10% M-5 both slightly increased with increasing SR. This finding is consistent with (Du et al., 2011) and may be attributed to the distance between the GNPs being higher than the critical maximum distance for electron hopping after biaxial deformation. Note no resistivity data was collected for PP/10% M-5 at SR = 2 due to the failure of the sample (rupture) during testing. It is worth mentioning that in a study conducted by You et al. (2017), enhanced electrical conductivity has been achieved by bi-axially stretching PP/Polymethylmethacrylate (PMMA)/GNP nanocomposites. In this case, GNP were firstly blended with PMMA and then mixed into PP matrix and PMMA bridged the GNP to the non-polar PP matrix, hence facilitating the homogeneous dispersion and the orientation of the chemically converted GNP during the stretching process. Shen et al. (2012) on the other hand, reported that the change of electrical conductivity in stretched PP/CNT composite film followed two stages. The electrical resistivity first increased up to $10^{11}\,\Omega\,cm$ (up to SR = 2.5), and further stretching the film (SR = 3.5) led to reduction of resistivity by eight orders of magnitude. Their results suggested an electrical percolation network rebuilding process following the breaking of the CNT conducting network.

After biaxially stretching, PP/GNP composites samples (SR1.5) were annealed at 150°C (below the T_m of PP). The volume resistivity decreased (conductivity increased) and returned to approximately the same value measured prior to stretching. The finding is in line with (Xiang et al., 2018) where post-deformation annealing is believed to allow polymer chain relaxation. As a consequence, increased contacts between the conductive filler materials can be achieved to re-establish the electrical percolation network. The electrical conductivity of the demonstrator parts, before or after annealing, showed consistent results to those obtained for biaxially stretched samples (SR1.5).

Microstructural Analysis (SEM)

Figure 4 shows the typical SEM images of unstretched PP/GNP 5% M-5 composite and the demonstrator part with the same composition produced from the vacuum thermoforming process. A homogeneous dispersion of GNP in the PP matrix can be observed on both sets of micrographs. The biaxial stretching effect caused by the thermoforming process is clearly visible in the demonstrator parts as the GNP are more dispersed and oriented along the diagonal direction (45° direction denoted by black arrows) as a result of stretching. This result is in line with previously reported bi-axially stretched polymer nanocomposites, where nanofillers such as CNT and nanoclay appear oriented in the stretching plane after biaxial stretching (Abu-Zurayk et al., 2010; Xiang et al., 2015).

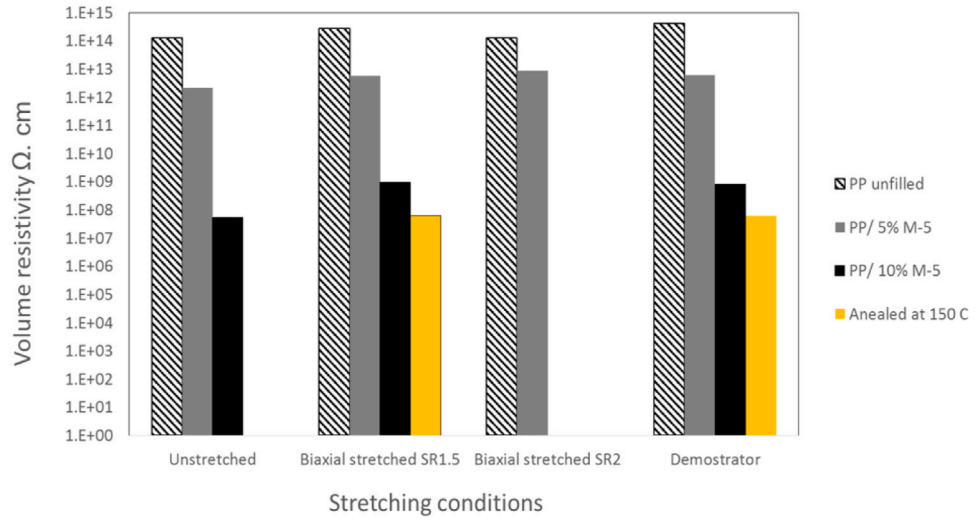

FIGURE 3 | Volume resistivity of unfilled PP, PP/GNP composites and their demonstrator parts.

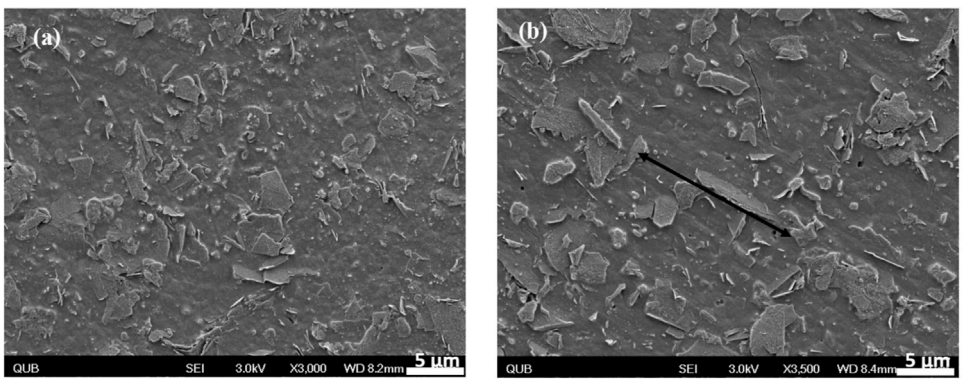

FIGURE 4 | SEM images of plasma etched **(A)** unstretched PP/GNP 5% M-5 and **(B)** the demonstrator part.

CONCLUSIONS

The effects of graphene nanoplatelet (GNP) addition and biaxial stretching on melt processed polypropylene (PP) and PP/GNP composites were investigated. Composite materials showed generally improved mechanical properties (Young's modulus and yield strength) as a result of GNP addition and biaxial stretching. The increased mechanical properties can be attributed to the increased polymer crystallinity and the greater restriction on molecular mobility. Thermal analysis of the stretched samples revealed a strain induced increase in crystallization. The volume resistivity of composites increased after biaxial stretching and with increasing SR, which is consistent with the disruption of GNP network pathways and increasing distance between GNP. However, the conductivity of stretched composites remained higher than unfilled PP, and annealing of the stretched specimens resulted in nearly full recovery of the conductivity prior to stretching. Further evaluation on the vacuum forming processed demonstrator parts showed similar thermal/mechanical and electrical properties comparable to those of the biaxially stretched (SR 1.5) samples. This confirms the biaxial stretching technique is capable of informing the structure and properties of the composites undergoing secondary processing such as vacuum forming.

This work provides the necessary platform for informed exploitation of polymer-graphene nanocomposites into processed articles, which will enable compounders, processors and designers of nanocomposite products to optimize the microstructure and properties of these materials to suit differing application requirements. The materials and processing techniques developed and utilized in this study have a wide range of potential applications such as low cost, light weight, electromagnetic insulating shielding and anti-static packaging, etc. Future work may be expanded to further explore the effect of biaxial stretching on wide range of polymer nanocomposite systems containing advanced functional

nanomaterials, such as CNT, graphene oxide, boron nitride nanosheets, tungsten disulphide (WS_2), molybdenum disulfide (MoS_2), etc.

DATA AVAILABILITY STATEMENT

The raw data supporting the conclusions of this article will be made available by the authors, without undue reservation.

AUTHOR CONTRIBUTIONS

BMa conducted the experiments. GM contributed to the bi-axial stretching experiment, PM contributed to the vacuum thermal forming experiments, GG contributed to the melt processing of polymer composites, BMi and PD contributed to the material characterization, AH and DS funding administration. All authors contributed to the results discussion/analysis, writing and revision of the manuscript.

FUNDING

Authors acknowledge QNRF NPRP award (NPRP5-039-2-014) (NRF) Qatar, Engineering and Physical Science Research Council (EP/M020851/1) for funding the research.

ACKNOWLEDGMENTS

The authors wish to thank the QNRF for research funding through NPRP award (NPRP5-039-2-014) (NRF) Qatar.The authors would also like to acknowledge the Engineering and Physical Science Research Council (EP/M020851/1) for funding support.

SUPPLEMENTARY MATERIAL

The Supplementary Material for this article can be found online at: https://www.frontiersin.org/articles/10.3389/fmats.2021.687282/full#supplementary-material

REFERENCES

Abu-Zurayk, R., Harkin-Jones, E., McNally, T., Menary, G., Martin, P., Armstrong, C., et al. (2010). Structure–property Relationships in Biaxially Deformed Polypropylene Nanocomposites. *Composites Sci. Techn.* 70 (9), 1353–1359. doi:10.1016/j.compscitech.2010.04.011

Beuguel, Q., Boyer, S. A. E., Settipani, D., Monge, G., Haudin, J-M., Vergnes, B., et al. (2018). Crystallization Behavior of Polypropylene/graphene Nanoplatelets Composites. *Polym. Crystallization* 1 (3), e10024. doi:10.1002/pcr2.10024

Díez, F. J., Alvariño, C., López, J., Ramírez, C., Abad, M. J., Cano, J., et al. (2005). Influence of the Stretching in the Crystallinity of Biaxially Oriented Polypropylene (BOPP) Films. *J. Therm. Anal. Calorim.* 81 (1), 21–25. doi:10.1007/s10973-005-0739-x

Du, J., Zhao, L., Zeng, Y., Zhang, L., Li, F., Liu, P., et al. (2011). Comparison of Electrical Properties between Multi-Walled Carbon Nanotube and Graphene Nanosheet/high Density Polyethylene Composites with a Segregated Network Structure. *Carbon* 49 (4), 1094–1100. doi:10.1016/j.carbon.2010.11.013

Feng, C., and Jiang, L. (2014). Micromechanics Modeling of Bi-Axial Stretching Effects on the Electrical Conductivity of CNT-Polymer Composites. *Int. J. Appl. Mech.* 07 (01), 1550005. doi:10.1142/S1758825115400050

He, M., Zhu, C., Xu, H., Sun, D., Chen, C., Feng, G., et al. (2020). Conducting Polyetheretherketone Nanocomposites with an Electrophoretically Deposited Bioactive Coating for Bone Tissue Regeneration and Multimodal Therapeutic Applications. *ACS Appl. Mater. Inter.* 12 (51), 56924–56934. doi:10.1021/acsami.0c20145

He, S., Zhang, J., Xiao, X., Hong, X., and Lai, Y. (2017a). Investigation of the Conductive Network Formation of Polypropylene/graphene Nanoplatelets Composites for Different Platelet Sizes. *J. Mater. Sci.* 52 (22), 13103–13119. doi:10.1007/s10853-017-1413-y

He, S., Zhang, J., Xiao, X., Lai, Y., Chen, A., and Zhang, Z. (2017b). Study on the Morphology Development and Dispersion Mechanism of Polypropylene/graphene Nanoplatelets Composites for Different Shear Field. *Composites Sci. Techn.* 153, 209–221. doi:10.1016/j.compscitech.2017.10.024

Jiang, Y., Yang, Y., Zheng, X., Yi, Y., Chen, X., Li, Y., et al. (2020). Multifunctional Load-Bearing Hybrid Hydrogel with Combined Drug Release and Photothermal Conversion Functions. *NPG Asia Mater.* 12 (1), 18. doi:10.1038/s41427-020-0199-6

Jun, Y-S., Um, J. G., Jiang, G., Lui, G., and Yu, A. (2018b). Ultra-large Sized Graphene Nano-Platelets (GnPs) Incorporated Polypropylene (PP)/GnPs Composites Engineered by Melt Compounding and its thermal, Mechanical, and Electrical Properties. *Composites B: Eng.* 133, 218–225. doi:10.1016/j.compositesb.2017.09.028

Jun, Y. S., Um, J. G., Jiang, G., and Yu, A. (2018a). A Study on the Effects of Graphene Nano-Platelets (GnPs) Sheet Sizes from a Few to Hundred Microns on the thermal, Mechanical, and Electrical Properties of Polypropylene (PP)/GnPs Composites. *Express Polym. Lett.* 12 (10), 885–897. doi:10.3144/expresspolymlett.2018.76

Kaszonyiová, M., Rybnikar, F., Kubišová, M., and Maňas, D. (2018). Effect of Beta Irradiation on the Structural Changes of Isotactic Polypropylene. *Materiali in tehnologije* 52 (1), 15–18. doi:10.17222/mit.2017.089

Kershah, T., Anderson, P. D., and van Breemen, L. C. A. (2020). Uniaxial and Biaxial Response of Anisotropic Polypropylene. *Macromolecular Theor. Simulations* 29 (4), 2000018. doi:10.1002/mats.202000018

King, J. A., Via, M. D., Morrison, F. A., Wiese, K. R., Beach, E. A., Cieslinski, M. J., et al. (2011). Characterization of Exfoliated Graphite Nanoplatelets/polycarbonate Composites: Electrical and thermal Conductivity, and Tensile, Flexural, and Rheological Properties. *J. Compos. Mater.* 46 (9), 1029–1039. doi:10.1177/0021998311414073

King, J. A., Tucker, K. W., Vogt, B. D., Weber, E. H., and Quan, C. (1999). Electrically and Thermally Conductive Nylon 6,6. *Polym. Composites* 20 (5), 643–654. doi:10.1002/pc.10387

Liang, J. Z., and Du, Q. (2018). Melt Flow and Flexural Properties of Polypropylene Composites Reinforced with Graphene Nano-Platelets. *Int. Polym. Process.* 33 (1), 35–41. doi:10.3139/217.3335

Maddah, H. A. (2016). Polypropylene as a Promising Plastic: A Review. *Am. J. Polym. Sci.* 6 (1), 1–11. doi:10.5923/j.ajps.20160601.0110.1155/2016/3478709

Martin, P. J., Tan, C. W., Tshai, K. Y., McCool, R., Menary, G., Armstrong, C. G., et al. (2005). Biaxial Characterisation of Materials for Thermoforming and Blow Moulding. *Plastics, Rubber and Composites* 34 (5-6), 276–282. doi:10.1179/174328905X64803

Mayoral, B., Garrett, G., and McNally, T. (2014). Effect of Screw Configuration Profiles on the Dispersion of MWCNTs in a Poly (Propylene) Matrix. *Macromolecular Mater. Eng.* 299, 748–756. doi:10.1002/mame.201300172

Mayoral, B., Harkin-Jones, E., Khanam, P. N., AlMaadeed, M. A., Ouederni, M., Hamilton, A. R., et al. (2015). Melt Processing and Characterisation of Polyamide 6/graphene Nanoplatelet Composites. *RSC Adv.* 5 (65), 52395–52409. doi:10.1039/C5RA08509H

Mayoral, B., Hornsby, P. R., McNally, T., Schiller, T., Jack, K., and Martin, D. J. (2013). Quasi-Solid State Uniaxial & Biaxial Deformation of PET/MWCNT Composites: Structural Evolution, Electrical and Mechanical Properties. *RSC Adv.* 3, 5162–5183. doi:10.1039/c3ra22597f

Nidamanuri, N., Li, Y., Li, Q., and Dong, M. (2020). Graphene and Graphene Oxide-Based Membranes for Gas Separation. *Engineered Sci.* 9, 3–16. doi:10.30919/es8d128906

Noorunnisa Khanam, P., AlMaadeed, M. A., Ouederni, M., Harkin-Jones, E., Mayoral, B., Hamilton, A., et al. (2016b). Melt Processing and Properties of Linear Low Density Polyethylene-Graphene Nanoplatelet Composites. *Vacuum* 130, 63–71. doi:10.1016/j.vacuum.2016.04.022

Noorunnisa Khanam, P., AlMaadeed, M. A., Ouederni, M., Mayoral, B., Hamilton, A., and Sun, D. (2016a). Effect of Two Types of Graphene Nanoplatelets on the Physico–Mechanical Properties of Linear Low–Density Polyethylene Composites. *Adv. Manufacturing: Polym. Composites Sci.* 2 (2), 67–73. doi:10.1080/20550340.2016.1235768

Shen, J., Champagne, M. F., Yang, Z., Yu, Q., Gendron, R., and Guo, S. (2012). The Development of a Conductive Carbon Nanotube (CNT) Network in CNT/polypropylene Composite Films during Biaxial Stretching. *Composites A: Appl. Sci. Manufacturing* 43 (9), 1448–1453. doi:10.1016/j.compositesa.2012.04.003

Singh, M. V. (2021). Conversions of Waste Tube-Tyres (WTT) and Waste Polypropylene (WPP) into Diesel Fuel through Catalytic Pyrolysis Using Base SrCO3. *Engineered Sci.* 13, 87–97. doi:10.30919/es8d1158

Tsai, P. (2020). Performance of Masks and Discussion of the Inactivation of SARS-CoV-2. *Engineered Sci.* 10, 1–7. doi:10.30919/es8d1110

Valentini, L., Biagiotti, J., Kenny, J. M., and López Manchado, M. A. (2003). Physical and Mechanical Behavior of Single-Walled Carbon Nanotube/polypropylene/ethylene–Propylene–Diene Rubber Nanocomposites. *J. Appl. Polym. Sci.* 89 (10), 2657–2663. doi:10.1002/app.12319

Xiang, D., Harkin-Jones, E., and Linton, D. (2015). Characterization and Structure–Property Relationship of Melt-Mixed High Density Polyethylene/multi-Walled Carbon Nanotube Composites under Extensional Deformation. *RSC Adv.* 5 (59), 47555–47568. doi:10.1039/C5RA06075C

Xiang, D., Wang, L., Zhang, Q., Chen, B., Li, Y., and Harkin-Jones, E. (2018). Comparative Study on the Deformation Behavior, Structural Evolution, and Properties of Biaxially Stretched High-Density Polyethylene/carbon Nanofiller (Carbon Nanotubes, Graphene Nanoplatelets, and Carbon Black) Composites. *Polym. Composites* 39 (S2), E909–E923. doi:10.1002/pc.24328

Xu, P., Qu, M., Ning, Y., Jia, T., Zhang, Y., Wang, S., et al. (2019). High Performance and Low Floating Fiber Glass Fiber-Reinforced Polypropylene Composites Realized by a Facile Coating Method. *Adv. Composites Hybrid Mater.* 2 (2), 234–241. doi:10.1007/s42114-019-00080-0

Yan, X., Liu, J., Khan, M. A., Sheriff, S., Vupputuri, S., Das, R., et al. (2020). Efficient Solvent-Free Microwave Irradiation Synthesis of Highly Conductive Polypropylene Nanocomposites with Lowly Loaded Carbon Nanotubes. *ES Mater. Manufacturing* 9, 21–33. doi:10.30919/esmm5f716

You, F., Li, X., Zhang, L., Wang, D., Shi, C-Y., and Dang, Z-M. (2017). Polypropylene/poly(methyl Methacrylate)/graphene Composites with High Electrical Resistivity Anisotropy *via* Sequential Biaxial Stretching. *RSC Adv.* 7 (10), 6170–6178. doi:10.1039/C6RA28486H

Yuan, D., Pedrazzoli, D., Pircheraghi, G., and Manas-Zloczower, I. (2017). Melt Compounding of Thermoplastic Polyurethanes Incorporating 1D and 2D Carbon Nanofillers. *Polymer-Plastics Techn. Eng.* 56 (7), 732–743. doi:10.1080/03602559.2016.1233265

Zhang, H-B., Zheng, W-G., Yan, Q., Yang, Y., Wang, J-W., Lu, Z-H., et al. (2010). Electrically Conductive Polyethylene Terephthalate/graphene Nanocomposites Prepared by Melt Compounding. *Polymer* 51 (5), 1191–1196. doi:10.1016/j.polymer.2010.01.027

Zhang, R-C., Huang, Z., Huang, Z., Zhong, M., Zang, D., Lu, A., et al. (2020). Uniaxially Stretched Polyethylene/boron Nitride Nanocomposite Films with Metal-like thermal Conductivity. *Composites Sci. Techn.* 196, 108154. doi:10.1016/j.compscitech.2020.108154

Zhao, S., Niu, M., Peng, P., Cheng, Y., and Zhao, Y. (2020). Edge Oleylaminated Graphene as Ultra-Stable Lubricant Additive for Friction and Wear Reduction. *Engineered Sci.* 9, 77–83. doi:10.30919/es8d807

Zhao, Y., Niu, M., Yang, F., Jia, Y., and Cheng, Y. (2019). Ultrafast Electro-Thermal Responsive Heating Film Fabricated from Graphene Modified Conductive Materials. *Engineered Sci.* 8, 33–38. doi:10.30919/es8d501

Zhou, Y., Wang, P., Ruan, G., Xu, P., and Ding, Y. (2021). Synergistic Effect of P[MPEGMA-IL] Modified Graphene on Morphology and Dielectric Properties of PLA/PCL Blends. *ES Mater. Manufacturing* 11, 20–29. doi:10.30919/esmm5f928

Zhu, S., Zhang, L., Sun, d., He, M., Tan, P., and Jiang, N. (2021). Graphene Reinforced Polyether Ether Ketone Nanocomposites for Bone Repair Applications. *Polymer Testing*, 107276. doi:10.1016/j.polymertesting.2021.107276

Conflict of Interest: Author MO was employed by the company Qatar Petrochemical Company.

The remaining authors declare that the research was conducted in the absence of any commercial or financial relationships that could be construed as a potential conflict of interest.